OPEN ACCESS

ACTA METALLURGICA SLOVACA

2020, VOL. 26, NO. 3, 104-110

RESEARCH PAPER

PROGRESSIVE CMT CLADDING FOR RENOVATION OF CASTING MOLD

Janette Brezinová [1]*, Miroslav Džupon[2], Ján Viňáš[1], Anna Guzanová[1], Viktor Puchý[2], Jakub Brezina[1], Dagmar Draganovská[1], Marek Vojtko[2]

[1] Department of Engineering Technologies and Materials, Faculty of Mechanical Engineering, Technical University of Košice, Mäsiarska 74, 040 01 Košice, Slovakia

[2] Institute of Materials Research, Slovak Academy of Sciences, Watsonova 47, 040 01 Košice, Slovakia

*Corresponding author: janette.brezinova@tuke.sk, tel.:+421556023542, Faculty of Mechanical Engineering, Technical university of Košice, 042 00, Košice, Slovakia

Received: 08.06.2020
Accepted: 30.07.2020

ABSTRACT

The paper presents the results of the research focused on the possibility of renewal of molded parts of molds in high-pressure casting of aluminum alloys by arc cladding. Two materials - Thermanit 625 and Thermanit X - were tested. Cladding layers were produced by CMT - Cold Metal Transfer technology in a protective atmosphere of Ar. The clad resistance in the molten melt of the aluminum alloy EN AB AlSi8Cu3 for 120 and 300 minutes was evaluated. Furthermore, ball-on-disc wear resistance of clads was assessed. The results were compared with the reference material - AISI / SAE 309 base tool steel.

Keywords: high pressure casting, cladding, high temperature corrosion, ball-on-disc

INTRODUCTION

High-pressure die casting technology (HPDC) is a balanced system of interrelations between the properties of aluminum alloy melt, the design of mold including the inlet and venting as well as conditions of mold cavity filling, in particular the melt velocity in mold and the hydrodynamic pressure [1]. Die-casting technology is a complex of interrelationships between alloy properties, mold design, and die casting operations. From the point of view of production efficiency and improvement of casting quality, besides technological parameters of die casting metal, the design solution of the mold and its technological service life are decisive. The technological service life of the mold is limited by the quality requirements prescribed for the casting and by the tolerance interval of the technological parameters for die casting. Molded parts and cores for aluminum alloy casting are usually made of chromium and chromium molybdenum tool steels. In the die casting process, molded parts and cores are subjected to intense thermal, mechanical and chemical loads. High melt flow rates of aluminum alloys (up to 120 $m.s^{-1}$), high pressures (up to 120 MPa) and high maximum surface temperatures of the molded parts (up to 550°C) lead to erosion, abrasion, corrosion and thermal fatigue of the mold. The heat load of the foundry cores is even higher (up to 600°C) because they are not connected to the mold cooling system. Thermal cyclic loading from 80°C to 550°C leads to high tensile stresses on the surface of mold, core moldings and consequently to the formation and propagation of thermal cracks. [2-4] Frequent contact of the molding surface with the melt causes the formation of build-ups (sticking) due to corrosion and consequently shortening the service life of the molding parts and cores. Any decomposition change of mold parts and cores will also affect the quality and dimensions of castings [5].

A key component of this technology is the mold and mainly its shape part - the mold inserts. The goal of the research is the renovation of surface which include arc cladding methods and are nowadays very actual. [6-9] Optimization of arc processes are oriented to reduce the heat input underlayer. [10-13] To reduce the number of defects and beginning of nucleation unwanted phases such as heterogenic areas. These are in the middle and high alloy steel located in heat affected zone under cladding layers. [14-17] One of the possibilities of restoring functional surfaces of injection molds or coremakers is with arc welding by CMT (Cold Metal Transfer) [18-20]. As an improvement of short circuit GMAW process, cold metal transfer (CMT) welding is characterized by low heat input, spatter free metal transfer, excellent gap-bridging ability and elegant bead formation. Molds renovated this way are heat-treated and machined to the required dimensions and surface quality. Latest published research on mold restoration by welding aims to identify ways and possibilities to increase mold surface lifetime using CMT welding and to verify the suitability of the chemical composition of newly developed additive materials for mold restoration [21-25].

During the production of aluminum castings, the aluminum melt comes into contact with the mold surface. It is necessary to ensure the correct filling of the mold cavity, the direction of metal flow in the mold cavity, so that its walls do not wear prematurely and to limit the local temperature rise, which would lead to excessive wear and deterioration of the surface cleanliness of the casting. The aim is to choose the mold material so as to ensure good wear resistance and a low coefficient of friction [26-36].

The aim of the research is testing of Ni and Fe based materials for purpose of HPDC mold restoration by CMT welding. Tests were focused on resistance of weld clads against dissolution in AlSi8Cu3 aluminum alloy melt and wear resistance.

MATERIAL AND METHODS

Cladding process

In the CMT process, when the electrode wire tip makes contact with the molten pool, the servomotor of the 'robacter drive' welding torch is reversed by digital process control. This causes the wire to retract promoting droplet transfer. During metal transfer, the current drops to near-zero and thereby any spatter generation is avoided. As soon as the metal transfer is completed, the arc is re-ignited and the wire is fed forward once more with set welding current reflowing [12, 22, 37].

A typical CMT welding electrical signal cycle can be defined as the period required to deposit a droplet of molten electrode into the weld pool. The analysis of current and voltage waveform is essential to study the energy distribution of different phases in droplet transfer process [38]. The cycle is divided into three phases as follows:

(i) The peak current phase: This is a constant arc voltage corresponding to a high pulse of current causing the ignition of the welding arc easily and then heats the wire electrode to form droplet.

(ii) The background current phase: The phase corresponds to a lower current. The current is decreased to prevent the globular transfer of the little liquid droplet formed on the wire tip. This phase continues until short circuiting occurs.

(iii) The short-circuiting phase: In this phase, the arc voltage is brought to zero. At the same time, the return signal is provided to the wire feeder which gives the wire a back-drawing force. This phase assists in the liquid fracture and transfer of material into the welding pool [39].

The complex waveform of the welding current in the CMT process and the 'back feeding' of the filler wire that mechanically forces the metal transfer make it difficult to understand the relation between welding parameters, metal transfer and heat transfer as shown in Fig.1. [22, 27]

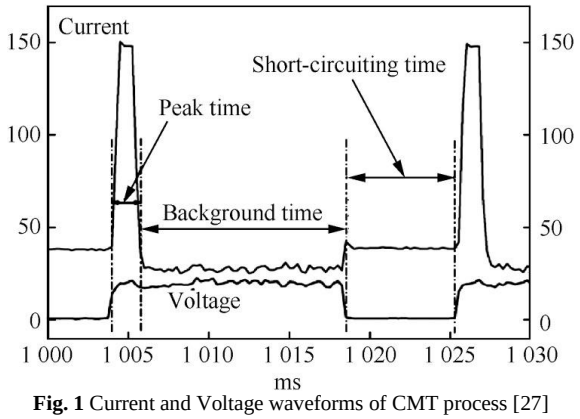

Fig. 1 Current and Voltage waveforms of CMT process [27]

Used filler material

Thermanit 625 (T 625) and Thermanit X (T X) welds were deposited on steel plates of 10 mm thick, made from AISI/SAE 309 (1.4828) steel using Fronius Trans Puls Synergic 5000 by CMT - Cold Metal Transfer welding machine in protection atmosphere of Ar. Welding parameters: 155 A, 16.5 V, 8.5 m.min^{-1}, wire feed 8 m.min^{-1}. Spectral chemical analyzer Belec Compact Port was used for chemical composition of basic material (BM) and weld clads. Chemical composition is given in Table 1. Mechanical properties of materials declared by material producer are shown in Table 2.

Table 1 Chemical composition of used materials, wt. % (Fe bal.)

	C	Mn	Si	Cr	V	Mo	Nb	Ni	Ti	Co
1.4828	0.075	0.41	1.15	19.48	0.06	0.07	-	13.92	0.01	0.035
T 625	0.004	0.86	0.56	20.42	0.01	8.13	3.1	bal.	0.004	0.004
T X	0.101	7.92	0.86	18.81	0.08	0.02	-	9.85	0.007	0.056

Table 2 Mechanical properties of used materials, average values

	YS [MPa]	UTS [MPa]	Elongation A_5 [%]
1.4828	260	500-750	30
T 625	420	760	30
T X	350	600	40

Immersion test

The test set a goal to simulate real operating conditions in HPDC mold and to find resistance of welds against dissolution in melt processed. Principle laid in immersion of BM and weld clads in the melt of aluminum alloy EN AB 46200-EN AB AlSi8Cu3(DIN EN 1706). Test coupons with dimensions of 20x20x10 mm were taken from BM and T 625 and T X welds. The aluminum alloy was embedded into ceramic crucibles and heated in a laboratory furnace to the melting point of the alloy. The temperature of alloy was maintained at 680±20°C temperature, which is a casting temperature of the alloy in HPDC machine with cold filling chamber. All weld samples were completely immersed in the melt in vertical position during the test for 120 and 300 minutes. After the time period, the samples were removed from the melt and cooled freely in the still air. On both surfaces of the samples, melt freely solidified and created a layer sticked on coupon surface. Coupons were next cut and metallographic sections were made for metallographic analyses using light optical microscope OLYMPUS GX71.
Interactions between the weld of T 625 and T X and solidified melt were observed by EDX microanalyses of element distribution after 120 and 300 minute exposure (680±20°C) using environmental scanning electron microscope SEM EVO MA15 with integrated analytical units EDX and WDX was used. For SEM analyses, regime SEI (Secondary Electron) with an accelerating voltage of 20 kV and a distance from the sample surface of 10 mm were used, and BSE (Backscaterred Electron) regime – allowing to observe chemical contrast.

Wear resistance test

Surfaces of welds were processed by grinding to a surface roughness Ra < 0.2 μm. Dry friction wear test (ball-on-disc) was performed on tribometer HTT, by CSM Instruments. Testing conditions: room temperature, 45% relative humidity, SiC ball of 6 mm in diameter, track radius varied from 3 to 7 mm, linear ball speed was 0.1 m.s^{-1}, the normal load Fp was 3N, 5N and 10N, respectively. During the test, tangential forces were measured, and friction coefficients were calculated. Wear tracks were subsequently observed by scanning electron microscopy and wear patterns, type of damage, and wear micromechanisms were identified. The mass losses of the materials were measured by the confocal profilomether and the specific wear rates (W) were calculated based on the volume loss (V) at the distances (L) and the normal load (Fp) according to ISO 20808.

RESULTS AND DISCUSSION

Metallographic sections through BM (Fig. 2 a) and a transition area to clad (Fig. 2 b, c) – solidified met interface. In both cases clads reacted with the aluminum alloy melt with different intensity, creating layer of reaction products on the phase interface.

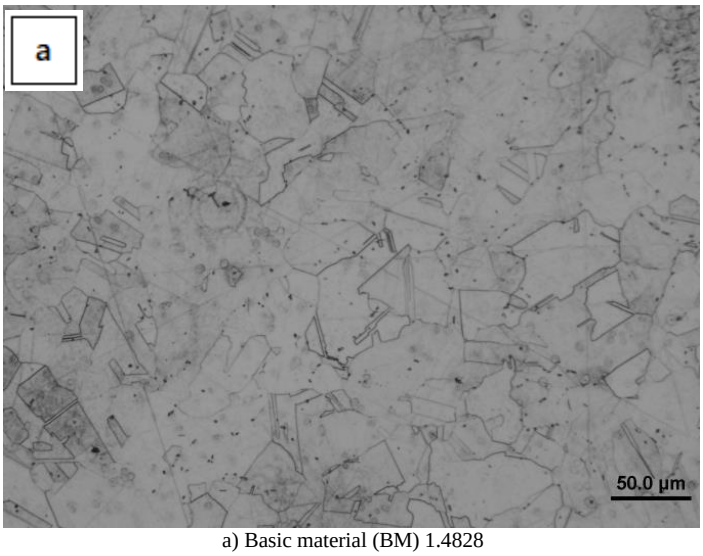

a) Basic material (BM) 1.4828

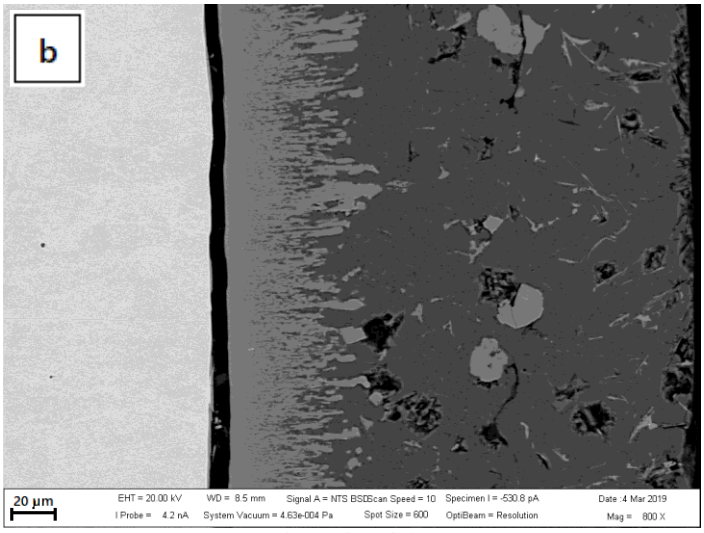

b) BM/680°C/300´/AlSi8Cu3

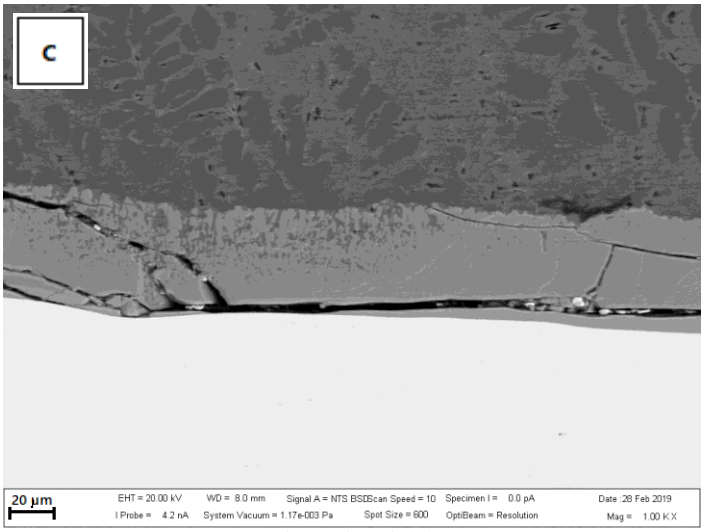

c) BM/680°C/120´/AlSi8Cu3

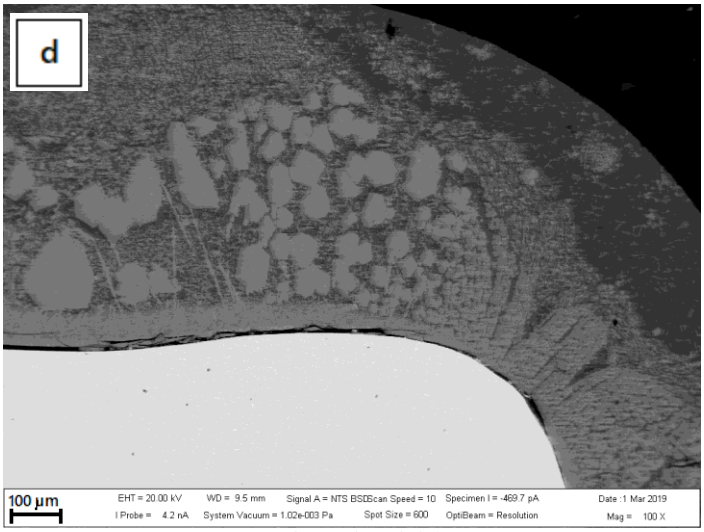

d) T 625/680°C/120´/AlSi8Cu3

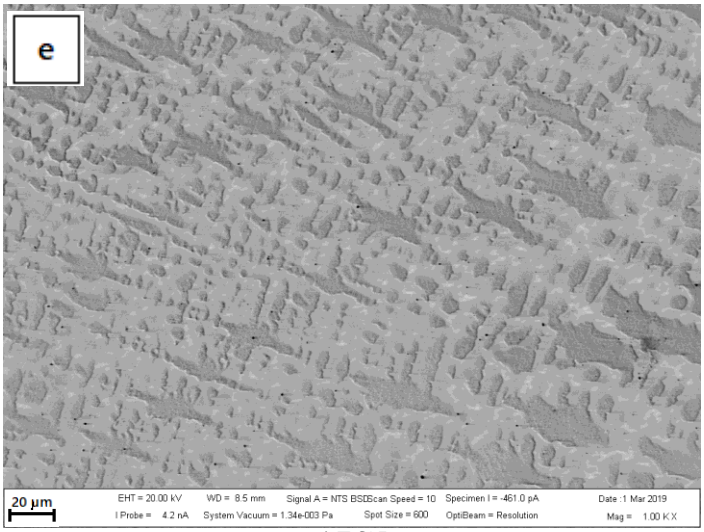

e) T 625

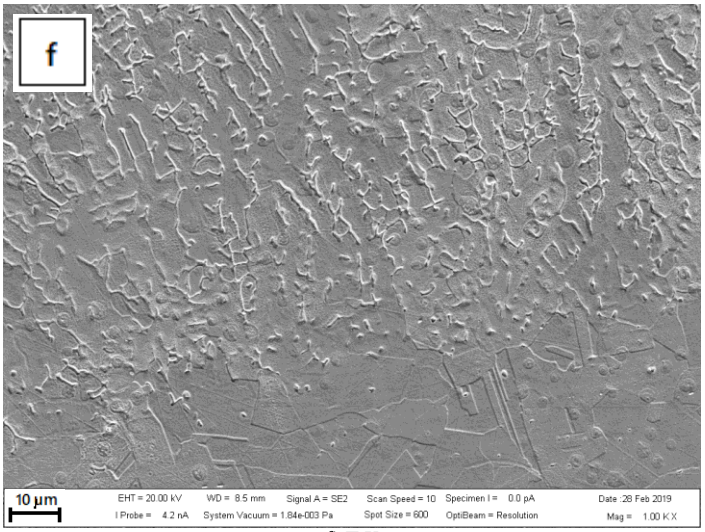

f) T X

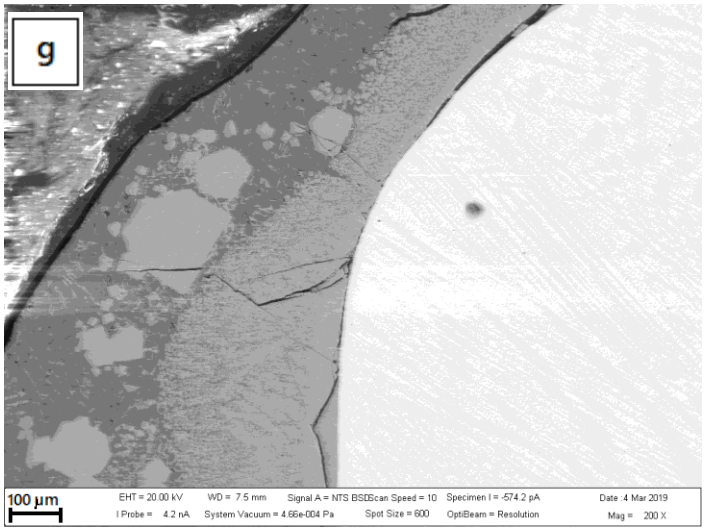

g) T 625/680°C/300´/AlSi8Cu3

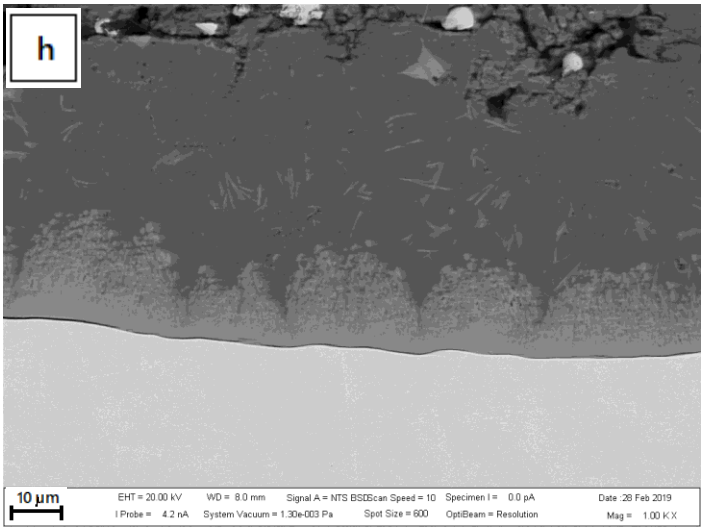

h) T X/680°C/120´/AlSi8Cu3

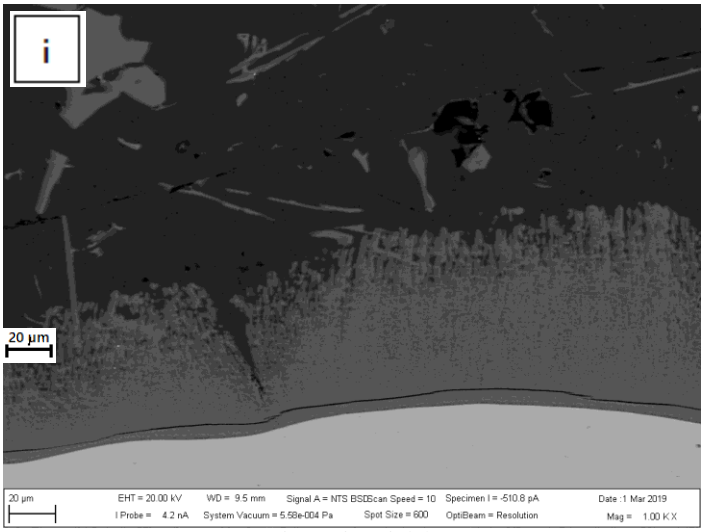

i) T X/680°C/300´/AlSi8Cu3

Fig. 2 Base material and clads T 625 and TX with full immersion in EN ABAlSi8Cu3 aluminum alloy at 680 ± 20 ° C for 120 and 300 min

Based on the microstructure of reaction products layer it can be stated that intense reaction of aluminum melt with T 625 clad took place at the areas of corners and edges of the samples (Fig. 2 d, g). The structure of the clads metal is shown in Fig. 2 e and f. Thickness of reaction products indicated higher resistance of T X clad (Fig. 2 h, i) and base material AISI/SAE 309 against dissolution in the aluminum alloy melt compared to the resistance of T 625 clad. During the 120 and 300 minute exposures of T 625 clad in the aluminum alloy melt a complex reaction of aluminum alloy EN AB AlSi8Cu3 with alloying elements present in the clads was observed. Using the qualitative elemental EDX microanalysis on the surface of the T 625 and T X clads an individual complex phase based on chromium, nickel, iron, molybdenum and niobium were observed in Fig. 3, result in Table 3. and Fig. 4, result in Table 4.

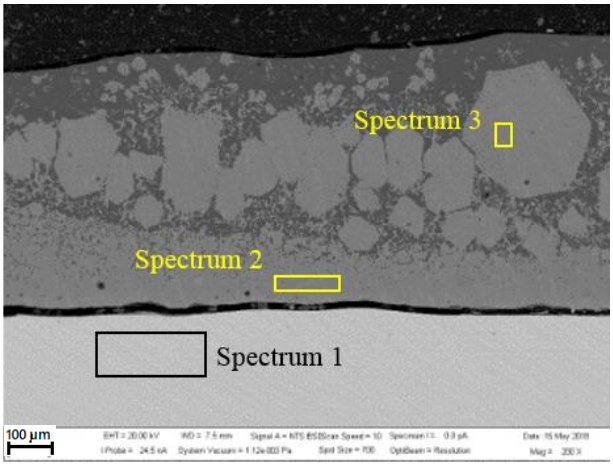

Fig. 3 Thermanit 625/680°C/300´/AlSi8Cu3 – area EDX semiquantitative microanalyses

Table 3 Thermanit 625/680°C/300´/AlSi8Cu3 – results EDX semiquantitative microanalyses

Spectrum 1		Spectrum 2		Spectrum 3	
Elem	Wt. [%]	Elem	Wt. [%]	Elem	Wt. [%]
Al	0.42	Al	53.02	Al	51.17
Si	0.44	Si	9.59	Si	10.89
Ti	0.20	Cr	12.98	Cr	14.40
Cr	21.98	Mn	0.33	Mn	0.58
Mn	0.40	Fe	10.32	Fe	14.15
Fe	15.29	Ni	8.75	Ni	3.39
Ni	52.68	Nb	1.40	Nb	1.05
Nb	2.50	Mo	3.62	Mo	4.37
Mo	6.11	Total	100	Total	100
Total	100				

Spectrum 1 confirms the chemical composition of the Ni deposit T 625 without diffusion of elements from the AlSi8Cu3 melt into the clad material. At the boundary of the deposit and the melt, Al, Si, Cr elements were detected in the solid state in concentrations corresponding to the composition of the melt, which formed the base of the compact interetallic layer. In the region formed by the solidified melt AlSi8Cu3 and the mixture of intermalic phases based on Al-Si-Nb-Cr-Fe, elements in the sense of spectrum 3 were detected.
The results of the chemical composition of the investigated areas are consistent with the chemical composition of the materials used. In the sub-clad layers (Spectrum 2), they correspond to the mixing of the additive material with the base material due to the used arc cladding technology.

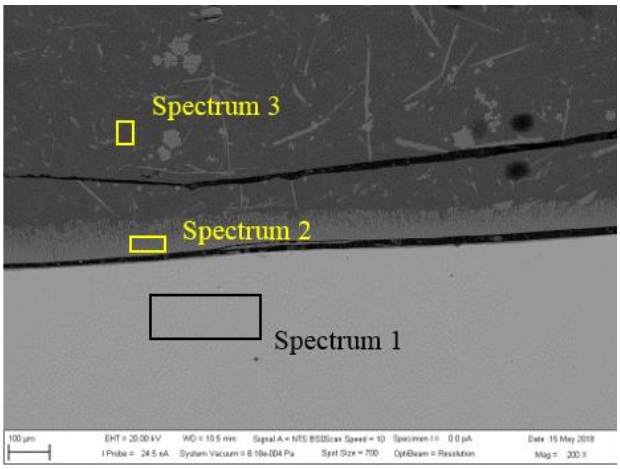

Fig. 4 Thermanit X/680°C/300´/AlSi8Cu3 – area EDX semiquantitative microanalyses

100 µm

Table 4 Thermanit X/680°C/300´/AlSi8Cu3 – results EDX semiquantitative microanalyses

Spectrum 1		Spectrum 2		Spectrum 3	
Elem	Wt. [%]	Elem	Wt. [%]	Elem	Wt. [%]
Si	1.03	Al	61.62	Al	57.05
Cr	19.93	Si	9.49	Si	14.52
Mn	6.06	Cr	7.18	Mn	0.58
Fe	64.15	Mn	1.77	Fe	27.19
Ni	8.83	Fe	19.93	Ni	0.66
Total	100	Total	100	Total	100

The T X cladding layers formed a reaction product based on Al-Fe-Si-Cr-Mn, spectrum 2. When comparing the compact phase formed on the clads, the Ni-based T 625 cladding layers has a higher tendency to dissolve in the melt. The melt resistance of the AlSi weld T X and the AISI 309 material is comparable with respect to the thickness of the compact layer of intermetallic compounds that have formed at the boundary. Thermal fatigue is a complex of physical and chemical interactions of a flowing melt in a mold cavity. A partial criterion by which we can qualitatively evaluate the resistance to thermal fatigue is the tendency to react the AlSi melt and the clad material. Based on the performed experiments, it is possible to hypothesize that the application of T 625 clad metal to the renovation of the mold surface will not increase the resistance to thermal fatigue due to the higher intensity of dissolution in the melt.

Wear resistance test

After a short initial stage, the course of friction coefficients was stable and reproducible (Fig. 5 a-c). Dependence of the specific wear rate (W) on applied load Fp is shown in Fig. 5 d.

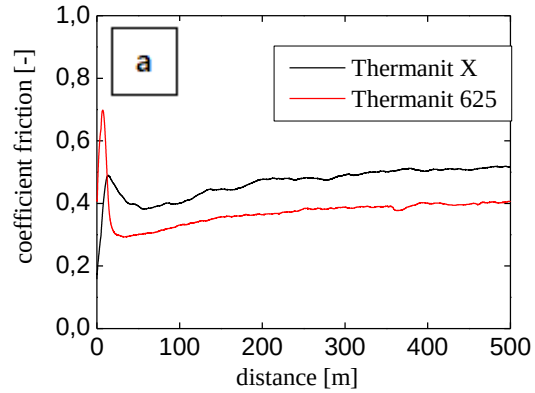

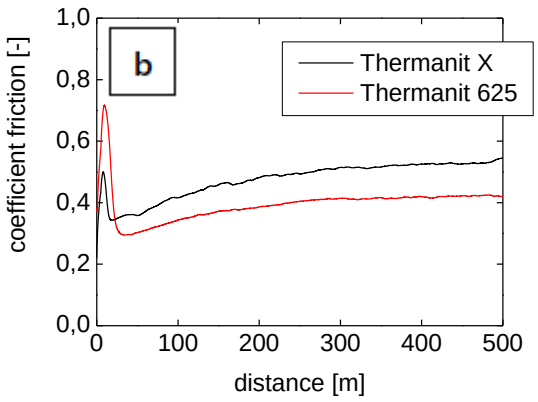

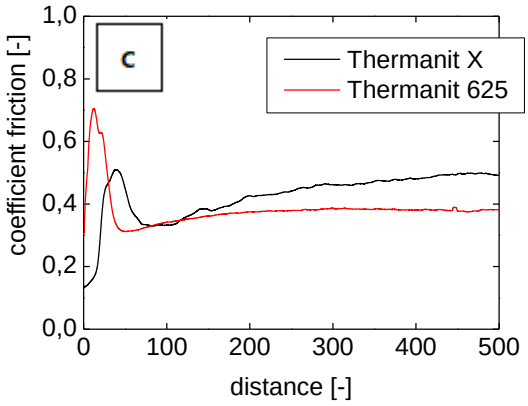

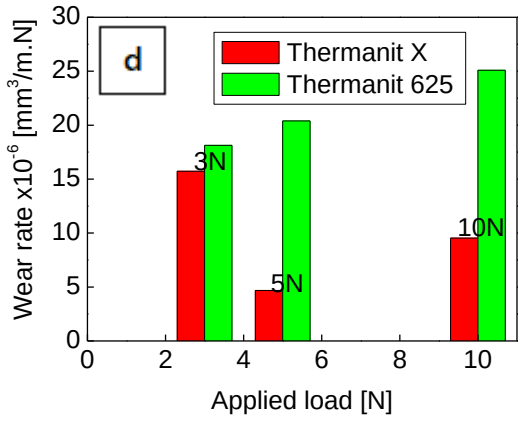

Fig. 5 Course of friction coefficients during tests at loads 3N (a), 5N (b) and 10N (c), dependence of specific wear rate (W) on applied load Fp (d)

Basic tribological characteristics of the clads T 625 and T X are listed in Table 5.

Table 5 Results of tribological test

Materials	Load Fp [N]	Wear track L [m]	Radius [mm]	COF [-] Start	Min.	Max.	Mean	Std. Dev.	Volume loss V [mm^3]	W [×10^{-6} mm^3/m.N]
T 625	3	500	3.0	0.41	0.28	0.75	0.37	0.051	0.0272	18.13
	5	500	4.5	0.38	0.29	0.75	0.40	0.059	0.0510	20.40
	10	500	6.5	0.30	0,29	0.75	0.38	0.062	0.1255	25.10
T X	3	500	7.0	0.16	0,16	0.54	0.47	0.045	0.0236	15.73
	5	500	3.0	0.22	0,22	0.55	0.48	0.057	0.0117	4.68
	10	500	5.0	0.14	0,13	0.55	0.43	0.072	0.0477	9.54

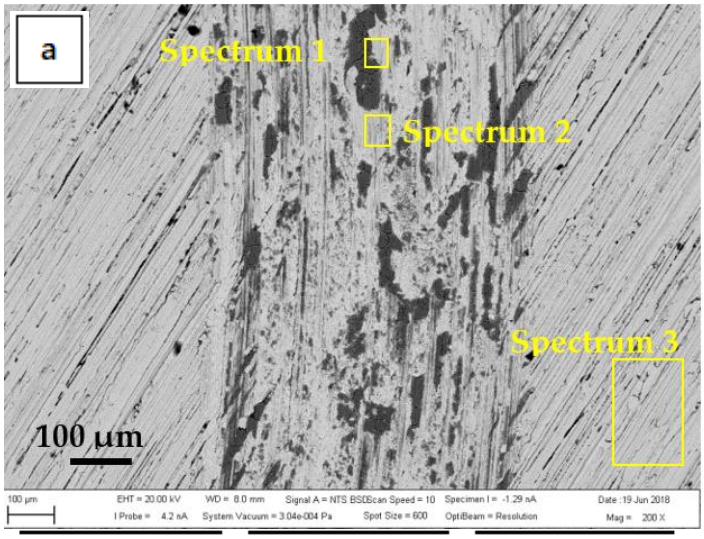

EDX spectrum 1		EDX spectrum 2		EDX spectrum 3	
Elem	Wt. [%]	Elem	Wt. [%]	Elem	Wt. [%]
O	31.89	O	6.59	O	2.13
Si	1.19	Al	0.17	Al	0.36
Ti	0.19	Si	0.88	Si	0.34
Cr	15.18	Ti	0.21	Cr	21.64
Fe	8.85	Cr	20.68	Mn	0.56
Ni	36.27	Mn	0.34	Fe	13.05
Nb	1.65	Fe	12.18	Ni	53.30
Mo	4.79	Ni	50.43	Nb	2.39
Total	100.00	Nb	2.46	Mo	6.23
		Mo	6.05	Total	100.00
		Total	100.00		

b

Fig. 6 Wear track at normal load 10 N: T 625, (a) EDX spectrum, (b) EDX analysis

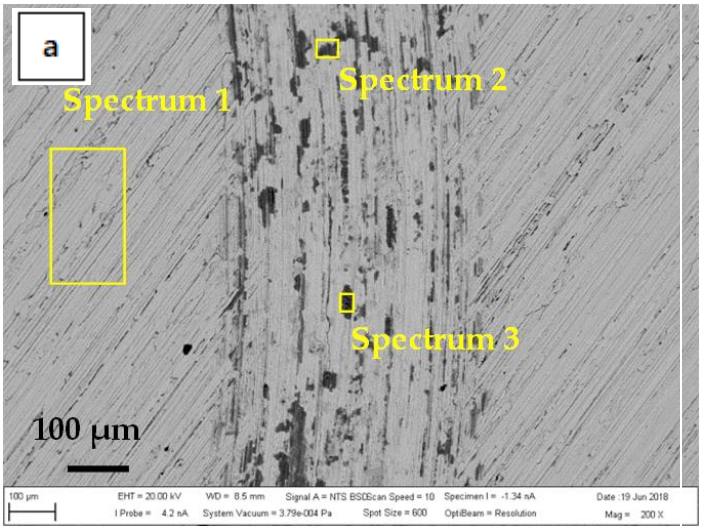

EDX spectrum 1		EDX spectrum 2		EDX spectrum 3	
Elem	Wt. [%]	Elem	Wt. [%]	Elem	Wt. [%]
O	1.57	O	24.62	O	32.88
Si	0.87	Si	2.74	Si	3.43
Cr	19.81	Cr	15.13	Cl	0.34
Mn	6.04	Mn	4.49	K	0.25
Fe	62.91	Fe	46.89	Ca	0.15
Ni	8.80	Ni	6.13	Cr	12.96
Total:	100.00	Total:	100.00	Mn	3.70
				Fe	40.74
				Ni	5.55
				Total:	100.00

b

Fig. 7 Wear track at normal load 10 N: (a) T X EDX spectrum, (b) EDX analysis

In Fig. 6 and 7 document the examined surface area after adhesive wear. The chemical composition at selected locations of the friction surface was determined by EDX analyzes. On the surface of the sample from T 625, the presence of Ni and Cr in particular was recorded in individual spectra. The elements T X san and the surface found elements Si, O and Cr.

CONCLUSION

Immersion test confirmed a complex reaction of aluminum alloy EN AB AlSi8Cu3 with alloying elements present in T 625 clad after 120 and 300 minute exposure especially in the area of corners and edges of the sample. Resistance of T X clad and underlying material AISI/SAE 309 in aluminum alloy melt was higher than the resistance of T 625 clad. Based on the experiments carried out it can be stated that the evaluated types of clads are not suitable for renovation of the shape parts of molds, because the elements are dissolved in contact with the aluminum alloy and degradation occurs in the areas of corners and edges. For this type of renovation a combination of clads and duplex PVD coating can be recommended. Adhesive wear was the dominant wear mechanism. T X and T 625 clad materials were pressed into the surface roughness of the static counterpart - SiC ball. The fragments of the intensively plastically deformed material T X and T 625 during the tribological test formed microbonds that were subsequently broken and formed a wear track pattern. The remains of the pressed material abraded the wear track. Part of energy generated during wear test was dissipated in tribo system and manifested by heat generation. As a result, the temperature of the tribo-couple increased locally. The intense plastic deformation of the surface of the tested clads and the local heating in the air created conditions for local oxidation of a part of the wear track. The complex of tribodegradation factors limiting the service life of functional surfaces is also affected by thermal fatigue. Ongoing cyclic tests of newly formed surfaces show an increase in thermal fatigue resistance of claded surfaces made with T 625 additive material, where the Ni matrix plays an important role, with high resistance to thermal influence. Against the base material, an increase in the resistance to thermal fatigue was also recorded on the cladding layers formed by the T X additive material.

Acknowledgments: This work was supported by scientific grant agency of the Ministry of Education of the Slovak Republic VEGA No. 1/0497/20, KEGA 001STU-4/2019 project of the Slovak Research and Development Agency APVV-16-0359 and the part of project Center for research of control of technical, environmental and human risks for permanent development of production and products in mechanical engineering (ITMS:26220120060).

REFERENCES

1. J. Hirsch: Transactions of Nonferrous Metals Society of China, 24(7), 2014, 1995-2002. https://doi.org/10.1016/S1003-6326(14)63305-7
2. V. Nunes et al.: Surface and Coatings Technology, 332(25), 2017, 319-331. https://doi.org/10.1016/j.surfcoat.2017.05.098
3. J. Viňáš et al.: Materials, 11(4), 2018, 1-13. https://doi.org/10.3390/ma11040459
4. Y. Zhu et al.: Materials Science and Engineering: A, 379(1-2), 2004, 420-431. https://doi.org/10.1016/j.msea.2004.03.020
5. J. Lin et al.: Surface and Coatings Technology, 201(6), 2006, 2930-2941. https://doi.org/10.1016/j.surfcoat.2006.06.024
6. J. Viňáš et al.: International Journal of Materials Research, 104(2), 2013, 183-191. https://doi.org/10.3139/146.110842
7. J. Brezinová et al.: Metals-Basel, 6(36) 2016, 1-12. https://doi.org/10.3390/met6020036
8. J. Brezinová et al.: Metals-Basel, 9(1232), 2019, 1-23. https://doi.org/10.3390/met9111232
9. J. Viňáš et al.: Materials Science Forum, 862, 2016, 41-48. https://doi.org/10.4028/www.scientific.net/MSF.862.41
10. J. Brezinová et al.: Metals-Basel, 10(164), 2020, 1-17. https://doi.org/10.3390/met10020164
11. P. Mohyla, K. Foldynová: Metal Science and Heat Treatment, 56, 2014, 206-209. https://doi.org/10.1007/s11041-014-9732-y
12. K. Furukawa: Welding International, 20(6), 2006, 440-445. https://doi.org/10.1533/wint.2006.3598
13. J. Viňáš et al.: Proceedings of the Institution of Mechanical Engineers, Part B: Journal of Engineering Manufacture, 227(12), 2013, 1841-1848. https://doi.org/10.1177/0954405413493405
14. J. Brezinová et al.: Key Engineering Materials, 586, 2014, 91-95, https://doi.org/10.4028/www.scientific.net/KEM.586.91
15. J. Viňáš et al.: Sadhana-Academy Proceedings In Engineering Sciences, 38, 2013, 477-490. https://doi.org/10.1007/s12046-013-0119-3
16. J. Viňáš et al.: Materials Science, 55(1), 2019, 46-51, https://doi.org/10.1007/s11003-019-00250-x
17. J. Viňáš et al.: Chemické listy, 105(17), 2011, 858-859.
18. J. González et al.: Procedia Manufacturing, 13, 2017, 840-847. https://doi.org/10.1016/j.promfg.2017.09.189
19. J. Viňáš et al.: Materials Science Forum, 862, 2016, 33-40. https://doi.org/10.4028/www.scientific.net/MSF.862.33
20. C.G. Pickin, S.W. Williams, M. Lunt: Journal of Materials Processing Technology, 211(3), 2011, 496-502. https://doi.org/10.1016/j.jmatprotec.2010.11.005
21. M. Marônek et al.: CMT welding of steel sheets treated by nitrooxidation In: *International Conference on Advances in Welding Science and Technology for Construction, Energy and Transportation: AWST 2010, held in Conjunction with the 63rd Annual Assembly of the International Institute of Welding: IIW 2010*: Istanbul: 11-17 July 2010 p. 773-777
22. S. Selvi, A. Vishvaksenan, E. Rajasekar: Defence Technology, 14(1), 2018, 28-44. https://doi.org/10.1016/j.dt.2017.08.002
23. B. Gungor, E. Kaluc, E. Taban, A. Sik: Materials and Design, 54, 2014, 207-211. https://doi.org/10.1016/j.matdes.2013.08.018
24. M. Student et al.: Strojnicky Casopis, 69(4), 2019, 133-146. https://doi.org/10.2478/scjme-2019-0048
25. V. Hutsaylyuk et al.: Vacuum, 2020, 109514, (in print). https://doi.org/10.1016/j.vacuum.2020.109514
26. C. Mitterer, F. Holler, F. Üstel, D. Heim: Surface & Coatings Technology, 125, (1-3), 2000, 233-239. https://doi.org/10.1016/S0257-8972(99)00557-5
27. A. Srivastava, V. Joshia, R. Shivpuria, R. Bhattacharya, S. Dixit: Surface & Coatings Technology, 163-164, 2003, 631-636. https://doi.org/10.1016/S0257-8972(02)00690-4
28. V. Hutsaylyuk et al.: Metals 2019, 9(280), 1-14. https://doi.org/10.3390/met9030280
29. A. Chaus et al.: Journal of Materials Engineering and Performance, 27, 2018, 3024-3034. https://doi.org/10.1007/s11665-018-3387-6
30. Y. Turygin et al.: Investigation of the electron beam positioning accuracy at electron beam welding. In.: *Procedia Engineering, International Conference on Manufacturing Engineering and Materials, ICMEM 2016, 6. - 10. June 2016*, Nový Smokovec, Slovakia, p. 489-494. https://doi.org/10.1016/j.proeng.2016.06.696
31. K. Bobzin, T. Brögelmann, U. Hartmann, N.C. Kruppe: Surface & Coatings Technology, 308, 2016, 374-382. https://doi.org/10.1016/j.surfcoat.2016.09.040
32. Ł. Tomaszewski et al.: Vacuum, 121, 2015, 223-229. https://doi.org/10.1016/j.vacuum.2015.08.027
33. B. Park, D.H. Jung, H. Kim, K.C. Yoo, J.J. Lee, J. Joo: Surface & Coatings Technology, 200(1-4), 2005, 726-729. https://doi.org/10.1016/j.surfcoat.2005.01.064
34. F.J.G. Silva, R.C.B. Casais, R.P. Martinho, A.P.M. Baptista: Journal of Nanoscience and Nanotechnology, 12, 2012, 9187-9194. https://pubmed.ncbi.nlm.nih.gov/23447976/
35. M.F.C. Andrade, R.P. Martinho, F.J.G. Silva, R.J.D. Alexandre, A.P.M. Baptista: Wear, 267(1-4), 2009, 12-18. https://doi.org/10.1016/j.wear.2008.12.114
36. J. Viňáš et al.: Journal of Adhesion Science and Technology, 27(2), 2013, 196-207. https://doi.org/10.1080/01694243.2012.701538
37. Z. Sun et al.: The International Journal of Advanced Manufacturing Technology, 80, 2015, 2007-2014. https://doi.org/10.1007/s00170-015-7197-9
38. J. Feng, H. Zhang and P. He: Materials and Design, 30(5), 2009, 1850-1852. https://doi.org/10.1016/j.matdes.2008.07.015
39. B. Mezrag, F. Deschaux-Beaume, M. Benachour: Science and Technology of Welding and Joining, 20(3), 2015, 189-198. https://doi.org/10.1179/1362171814Y.0000000271